FORUM GEOGRAFI
ISSN: 0852-0682 | E-ISSN: 2460-3945

HTTPS://JOURNALS.UMS.AC.ID/INDEX.PHP/FG/

Research article

Assessment of Soil Salinity in Arid Regions Using Remote Sensing and Machine Learning Models: Evidence from Karakalpakstan

Bekmurat Abdikairov[1], Mukhiddin Juliev[2,3,4,*], Madinabonu Kholmurodova[5], Zilolakhon Djanpulatova[2], Zuhra Khadjieva[2], Sojidabonu Turdalieva[2]

[1] Institute of Agriculture and Agrotechnologies of Karakalpakstan, Nukus, 230109, Uzbekistan; [2] Institute of Fundamental and Applied Research at (TIIAME) National Research University, Tashkent, 100000, Uzbekistan; [3] Turin Polytechnic University in Tashkent, Tashkent, 100095, Uzbekistan; [4] Tashkent State Technical University, Tashkent, 100095, Uzbekistan; [5] Tashkent Institute of Irrigation and Agricultural Mechanization Engineers, National Research University, Tashkent, 100000, Uzbekistan.

[*)] Correspondence: mukhiddinjuliev@gmail.com

Citation:
Abdikairov, B., Juliev, M., Kholmurodova, M., Djanpulatova, Z., Khadjieva Z., & Turdalieva, S. (2026). Assessment of Soil Salinity in Arid Regions Using Remote Sensing and Machine Learning Models: Evidence from Karakalpakstan. Forum Geografi. 41(1), 129-144.

Article history:
Received: 22 May 2026
Revised: 17 September 2026
Accepted: 18 September 2026
Published: 18 September 2026

Abstract

Soil salinization is a major environmental challenge in arid and semi-arid regions, reducing agricultural productivity and threatening sustainable land management. The spatiotemporal dynamics of soil salinity in the Shimbay district (Republic of Karakalpakstan, Uzbekistan) were investigated using multi-temporal Sentinel-2 imagery and the performance of Partial Least Squares Regression (PLSR), Random Forest (RF), and Multiple Linear Regression (MLR) models was compared. Soil salinity was assessed using the Normalized Difference Salinity Index (NDSI), Normalized Difference Vegetation Index (NDVI), Soil Moisture Index, and land surface temperature, together with field-measured soil electrical conductivity. The results revealed considerable interannual variability in soil salinity, with NDSI values ranging from 0.011 to 0.058 during 2018–2025 and an increasing salinity trend in 2024–2025. Among the evaluated models, PLSR achieved the highest predictive accuracy (R2 = 0.934, root mean square error (RMSE) = 0.398, mean absolute error (MAE) = 0.329), outperforming RF (R2 = 0.810) and MLR (R2 = 0.677). These findings demonstrate that integrating Sentinel-2-derived spectral indices with advanced modeling techniques provides an effective approach for assessing regional soil salinity. The proposed framework offers valuable support for sustainable land and water management in arid agricultural regions. However, further validation using larger datasets and broader environmental conditions is recommended.

Keywords: salinity mapping, geospatial modeling, soil degradation, Sentinel-2, environmental monitoring, predictive modeling.

1. Introduction

Soil salinization is a prevalent form of soil degradation, particularly in arid and semi-arid environments, which jeopardizes agricultural output, ecosystem functionality, and food security (Abou Samra & Ali, 2018; Nurmemet *et al*., 2018; Rengasamy, 2010). Salinity and sodicity have affected over one billion hectares of land globally, chiefly as a result of intense irrigation, elevated evapotranspiration, and insufficient drainage (Etesami & Noori, 2019; Ivushkin *et al*., 2019). Salt accumulation deteriorates the physical and chemical properties of soil, impedes plant water absorption, diminishes crop yields, and results in significant economic losses in irrigated agriculture (Qadir *et al*., 2014; Shrivastava & Kumar, 2015). Moreover, soil salinization has been recognized as a significant factor contributing to the reduction of global terrestrial production, exerting a more substantial influence than urbanization on net primary production (Wang *et al*., 2023).

Soil salinization has a particularly severe impact on irrigated agricultural areas. Central Asia, particularly the Aral Sea Basin, is one of the most vulnerable regions to secondary salinization due to long-term irrigation practices, inadequate water management, and climate-driven hydrological shifts (Micklin, 2007). Soil salinity has become a serious environmental and agricultural concern in Uzbekistan, especially in the Republic of Karakalpakstan, negatively affecting crop output, land quality, and irrigation efficiency (Djanibekov & Finger, 2018; Dubovyk *et al*., 2013). As a result, the precise and timely monitoring of soil salinity dynamics is critical for promoting sustainable land management, increasing agricultural production, and enhancing climate adaptation efforts.

Traditionally, soil salinity was determined through field observations, typically by measuring the electrical conductivity (EC) of soil samples collected for laboratory analysis. Although these approaches provide valid point-based data, they are labor-intensive, time-consuming, costly, and frequently provide limited spatial coverage, particularly across large agricultural areas (Allbed *et al*., 2014; Corwin *et al*., 2007; Muhetaer *et al*., 2022). Optical remote sensing has become a viable alternative to overcome these limitations because of its large spatial coverage, frequent observations, and cost-effectiveness (Wang *et al*., 2022). Multispectral satellite missions, particularly Landsat and Sentinel-2, have been widely used to detect and map soil salinity using vegetation- and salinity-related spectral indices, such as the Normalized Difference Vegetation Index (NDVI), Salinity Index, and Normalized Difference Salinity Index (NDSI) (Taghadosi *et al*., 2019; Thangarasu *et al*., 2025). Recent studies have improved salinity evaluation by combining Sentinel-2-derived spectral data with field observations and environmental variables (Sahbeni, 2021; Z. Wang *et al*., 2021). However, these techniques may be constrained by the intricate relationships among the vegetation condition, soil moisture, meteorological conditions, and spectral responses.

Recent advances in remote sensing and geospatial analytics have transformed soil salinity evaluation from traditional spectral index approaches to machine learning (ML) algorithms capable of modeling complex non-linear interactions between environmental variables and soil salinity (Aihaiti *et al*., 2025; Wang *et al*., 2024; Xiao *et al*., 2024). Algorithms such as random forest (RF), support vector machine, extreme gradient boosting (XGBoost), and artificial neural networks (ANN) have proven outstanding predictive abilities compared to conventional statistical techniques by effectively integrating spectral, topographic, and environmental predictors (Aksoy *et al*., 2022; Mohamed *et al*., 2023; Sulieman *et al*., 2023; Taghizadeh-Mehrjardi *et al*., 2021; Wang *et al*., 2021). Sentinel-1 Synthetic Aperture Radar (SAR) and Sentinel-2 multispectral imaging have been used in recent studies to increase the reliability of soil salinity mapping under various environmental conditions (Golestani *et al*., 2023; Mirzaee *et al*., 2024). Recently, both deep learning and explainable artificial intelligence (XAI) techniques have emerged as potential approaches to boost model accuracy and interpretability (Das *et al*., 2023; Jia *et al*., 2024; Zhang *et al*., 2025). These developments indicate the rapid advancement of data-driven approaches for soil salinity evaluation, while highlighting the need for additional regional validation (Shi *et al*., 2022; Wang *et al*., 2024).

Despite significant advances in soil salinity evaluation using spectral indices and ML, important challenges remain, particularly in Central Asia's arid irrigated zones. Most earlier research has focused heavily on traditional statistical techniques or spectral index-based evaluations, which may fail to sufficiently represent the complicated non-linear interactions between ecological factors and soil salinity levels (Amir Latif *et al*., 2025; Sarkar *et al*., 2023). Essentially, ML methodologies, such as RF and support vector machines, have demonstrated potential for enhancing salinity forecasting precision; however, comparative assessments of ML and regression-based algorithms remain constrained in the Republic of Karakalpakstan and the Aral Sea region (Duan *et al*., 2022; Ibrakhimov *et al*., 2020). Furthermore, limited research has examined the efficiency of integrating remotely detected spectral characteristics with field measurements for local-scale salinity evaluation under Uzbekistan's particular ecological and weather conditions. As a result, regional-specific and rigorous modeling systems designed for increasing soil salinity forecasting and promoting sustainable agriculture regulation in ecologically susceptible irrigated areas are still in demand.

Thus, the primary goal of this research is to investigate the potential of remote sensing data and statistical ML methodologies for soil salinity monitoring in the Republic of Karakalpakstan, Uzbekistan. The study's particular objectives are to: 1) evaluate the soil salinity dynamics of croplands using Sentinel-2 (surface reflectance) by spectral indices; 2) investigate the influencing factors for the salinity process, such as moisture, drought, and land surface temperature; and 3) analyze different models of soil salinity, such as RF, MLR, and partial least. Square Regression. The results of this study are expected to help create reliable and affordable techniques for soil salinity tracking and sustainable land management in climate-sensitive locations.

2. Methods

2.1. Study Area

The study area (Shimbay district) is situated in the northwestern part of Uzbekistan (Figure 1) along the Kegeyli Channel, on the right lower riches of the Amu Darya River in the front part of the Aral Sea delta, covering a 1405 km^2 area. It is located between 43°20′20.338″N and 59°58′16.041″E (Jumaniyazov et al., 2026). Shiba district is characterized as a flat plain with an absolute elevation of 52–67 m. The climate of the region is sharply continental with a long summer period (+40–45˚C) and a short winter period (−10–12˚C), where the groundwater level is close to the Earth's surface. The annual precipitation is 100 mm, while evaporation exceeds 2400 mm, demonstrating a typical arid zone. Groundwater is typically shallow and close to the land surface, promoting the capillary rise of saline groundwater and accelerating salt deposition in the root zone.

The district's agricultural territory is dominated by irrigated croplands fed by the Kegeyli Canal, which are largely used for growing for wheat, rice, maize, and pasture. Alluvial meadows and meadow-alluvial soils have low organic matter content and are highly susceptible to secondary salinization under long-term irrigation (Jumaniyazov *et al*., 2024). Insufficient natural drainage and an inefficient drainage network contribute to waterlogging and soluble salt accumulation in agricultural areas. Soil salinity is one of the most significant environmental restrictions to agricultural productivity in the region, with moderately and extremely saline soils found across vast expanses of irrigated agriculture. The natural vegetation consists primarily of desert shrubs and sparse halophytic species adapted to saline and arid conditions.

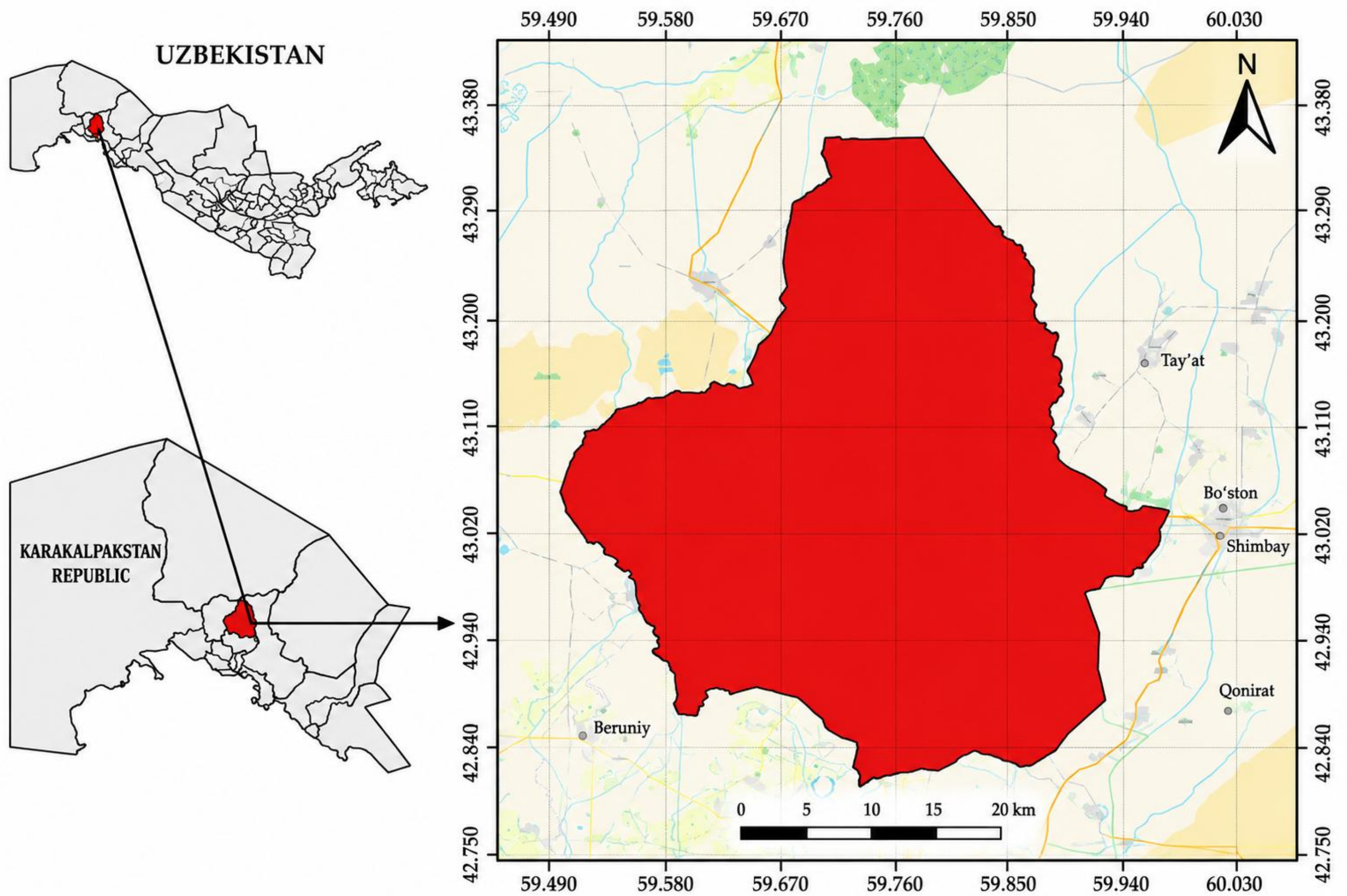

Figure 1. Location of the study area (Shimbay district, Republic of Karakalpakstan, Uzbekistan).

2.2. Remote Sensing Data Processing

Satellite image processing was conducted using the cloud-based Google Earth Engine (GEE) platform. Sentinel-2 Level-2A surface reflectance imagery from the COPERNICUS/S2_SR_HARMONIZED collection was used to construct a multi-temporal dataset from 2017 to 2025. Images were selected for the main growing season (1 April–31 October) to represent the period of maximum vegetation activity and agricultural development in the Shimbay district.

The image collection was filtered using the CLOUDY_PIXEL_PERCENTAGE metadata filter according to three criteria: (i) the boundary of the study area, (ii) the specified growing season for each year, and (iii) cloud contamination. Images exceeding the predefined cloud threshold were excluded to minimize atmospheric effects. Annual seasonal median composites were then generated from all cloud-filtered Sentinel-2 images acquired during the growing season to reduce residual cloud contamination and provide a consistent spectral representation of the study area.

Following image preprocessing, the Sentinel-2 spectral bands were used to derive the predictor variables employed in the modeling process. These included vegetation, salinity, and soil moisture indices, namely, the NDVI, NDSI, and soil moisture index (SMI). All predictor layers were generated at a spatial resolution of 10 m and exported in the GeoTIFF format using the WGS84 geographic coordinate system (EPSG:4326).

Field observations consisted of 20 sampling locations where soil EC was measured to represent soil salinity. The predictor values extracted from the satellite-derived layers were linked with the corresponding EC measurements to establish the modeling dataset used for statistical analysis.

Three modeling approaches were evaluated for soil salinity prediction: MLR, RF, and PLSR. The model performance was assessed using the coefficient of determination (R^2), root mean square error (RMSE), and mean absolute error (MAE). All image preprocessing, predictor extraction, statistical analyses, and model implementation were performed using the cloud-based GEE platform (Google LLC, Mountain View, CA, USA), while QGIS (version 3.34, QGIS Development Team, Open Source Geospatial Foundation, Beaverton, OR, USA) was used for spatial visualization and map preparation. Subsequently, the processed satellite dataset and derived predictor variables were used to analyze the spatial and temporal dynamics of soil salinity and evaluate the predictive performance of the selected modeling approaches across the agricultural lands of the Shimbay district.

2.3. Land Cover Map

To identify the land cover classes of Shimbay district for soil salinity assessment of croplands, the European Space Agency (ESA) WorldCover dataset with 10-meter spatial resolution was obtained. According to Zanaga *et al*., (2021), the land cover map from ESA WorldCover has 11 classes. Based on these data, a land use and land cover map of the study area was developed. Due to the natural environmental conditions and the time frame for space images, the study area contained only 8 classes of land cover maps, as shown in Figure 2.

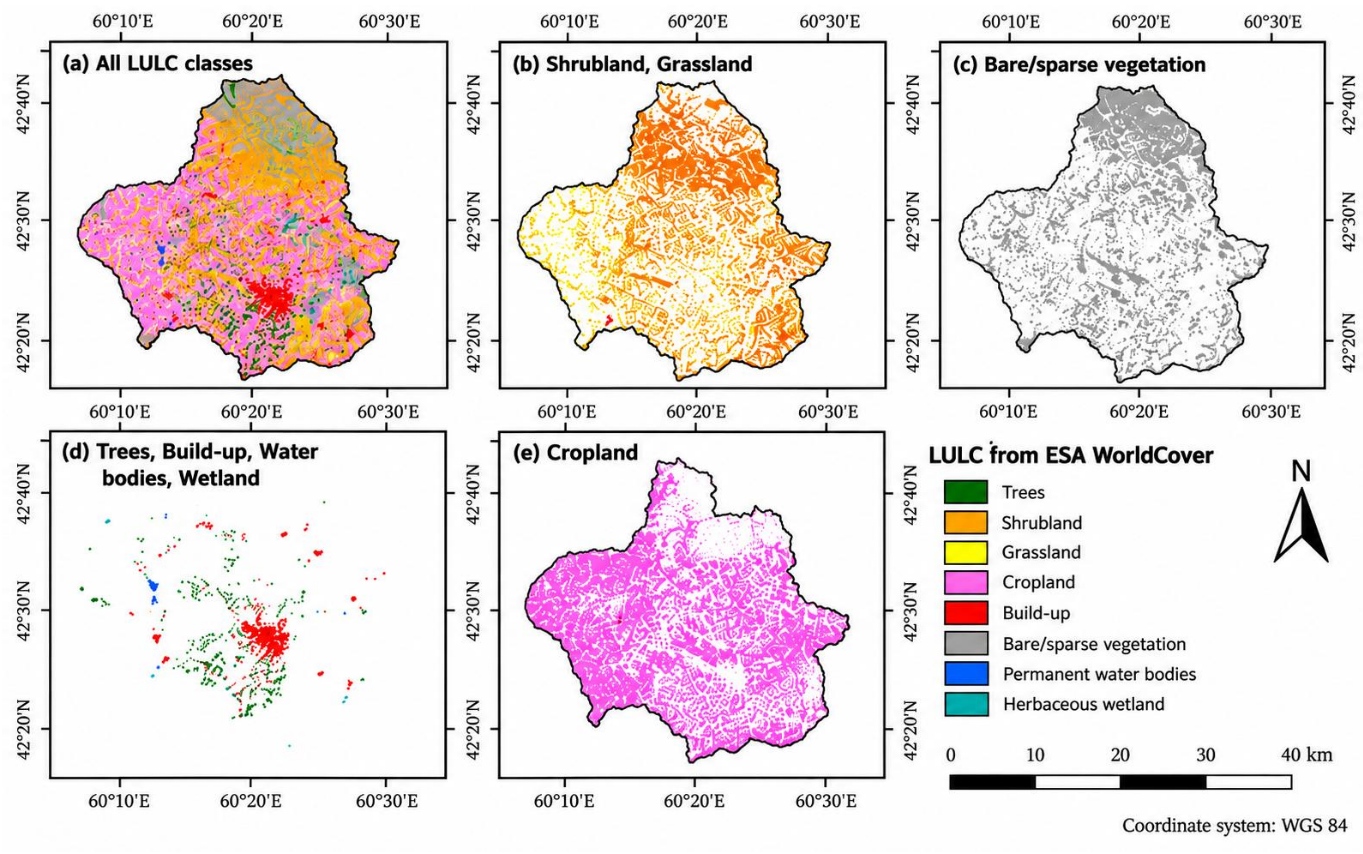

Figure 2. Land cover map of the Shimbay district derived from ESA WorldCover 2021 at a spatial resolution of a 10 m.

2.4. Soil Sample Collection and Analysis

As recognized by Avdan *et al*., (2022) and Khongnawang *et al*., (2022) to regulate soil salinity, foundational data are essential, especially regarding the geographic dispersion of the electrical conductivity of a saturated soil paste (ECe − ds/m). According to investigations of Farahmand & Sadeghi, (2020), the EC values of saline soils typically exceed 4 dS/m. Soil samples were obtained from 20 locations (0–30 cm) in November 2025, which were uniformly distributed among agricultural fields covering a 758 km^2 area (Figure 3). The collected samples were derived from agricultural lands cultivated with corn, rice, and wheat, and EC was measured at the laboratory of the Institute of Agriculture and Agrotechnologies of Karakalpakstan.

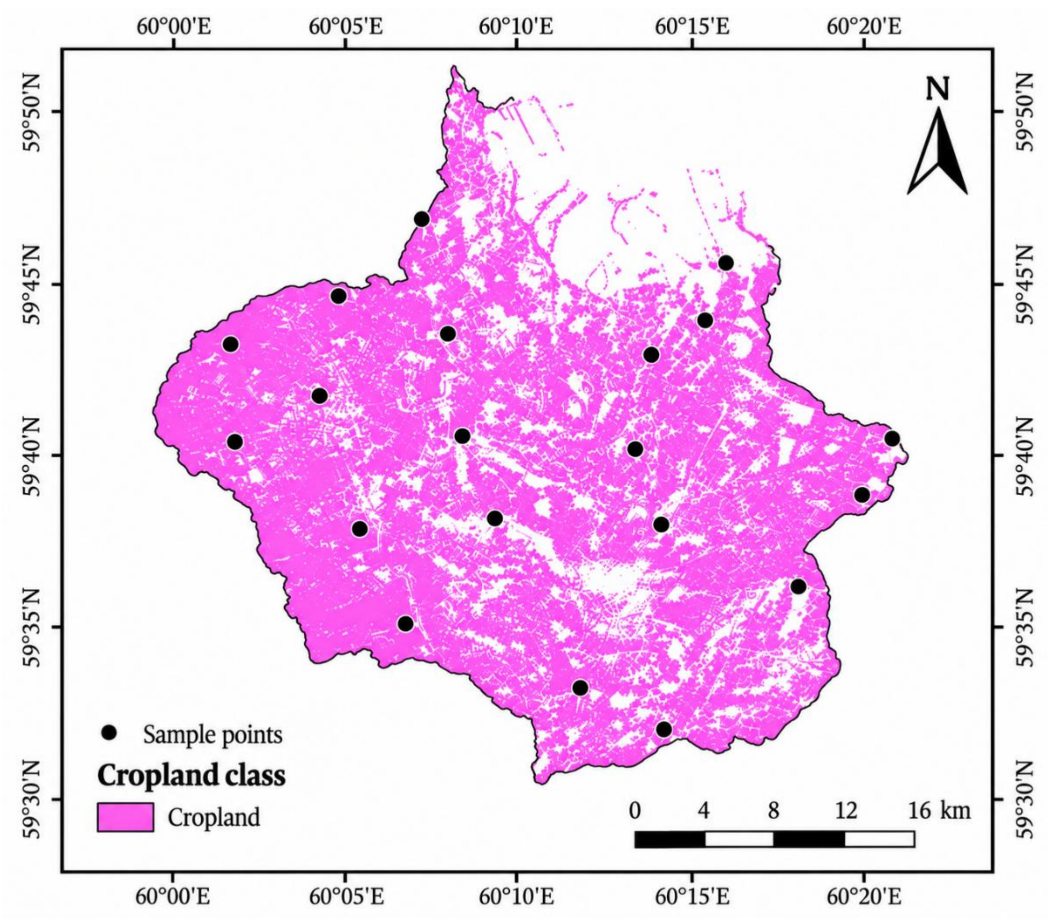

Figure 3. Distribution of soil sampling locations across the agricultural lands of the Shimbay district used for soil electrical conductivity (EC) measurements.

2.5. Model Development

Based on the literature review, a previous study on soil salinity modeling assessment (Abdikairov *et al*., 2024) identified the most appropriate models for soil salinity assessment including Multiple Linear Regression (MLR), RF and Partial Least Square Regression (PLSR). These models were chosen because they reflect typical statistical regression, multivariate regression, and ML methodologies used in soil salinity research based on remote sensing.

MLR was used as a standard statistical method to assess the linear correlations between soil EC and specific spectral characteristics acquired from Sentinel-2 data. The MLR model, which predicts soil salinization as a linear combination of predictor factors, is often employed in ecological and soil research because of its clarity and convenience. MLR is an easy-to-understand method that can be implemented rapidly and efficiently without requiring significant ML techniques (Ngabire *et al*., 2022). A linear equation is used to predict the relationship between many explanatory variables and a response variable (Shahabi *et al*., 2017). The relationship between predictors and EC in the models is described by Equation 1, which was developed by Taghadosi *et al*. (2019). where y_i is a model-estimated parameter correlated with EC outcomes. The K predictor elements $(X_{1,i}, X_{2,i} \dots, X_{k,i})$ indicates satellite feature indices. The unknown coefficients $(a_1, a_2 \dots, a_k)$ are found during the analysis, while e_i represents the error component for every data point.

$$EC = y_i = a_0 + a_1X_{1,i} + a_2X_{2,i} + a_3X_{3,i} + \cdots + a_kX_{k,i} + e_i \quad (1)$$

PLSR was employed to address potential convergence and multidimensionality difficulties using spectral predictors. PLSR reduces the number of initial variables to fewer implicit components while increasing the correlation between prediction factors and responses. This approach is most successful when the spectral bands and indices have a high intercorrelation coefficient and the total number of forecasters is greater than the number of samples. The PLSR model technique applies a simple multidimensional structure to link two separate data matrix variables: the variable of prediction X and the variable of responder Y (Nawar *et al*., 2014). According to Sahbeni (2021), PLSR facilitates the integration of spectral bands and spectral enhancers derived from the same image into a unified model, thus mitigating the collinearity problem prevalent in conventional regression analysis.

RF, a non-parametric group ML approach, was used to record the intricate non-linear interactions between spectral features and soil salinity. RF creates numerous choice trees from bootstrapping examples and randomly selected subsets of predictor parameters. The final projection is formed by combining the results of each tree. The RF model is well-known for its resistance to overfitting, capacity to manage non-linear responses, and superior prediction accuracy in ecological modeling scenarios. RF is a type of supervised ML that is effective for addressing regression and classification issues while identifying non-linear correlations between the desired outcome and input parameters (Zarei *et al*., 2021). In many cases, it has been applied to evaluate soil salinity, including in the Tarim Basin of China, based on its well-established proficiency in managing excessive dimension and interference in input information (Ma *et al*., 2017).

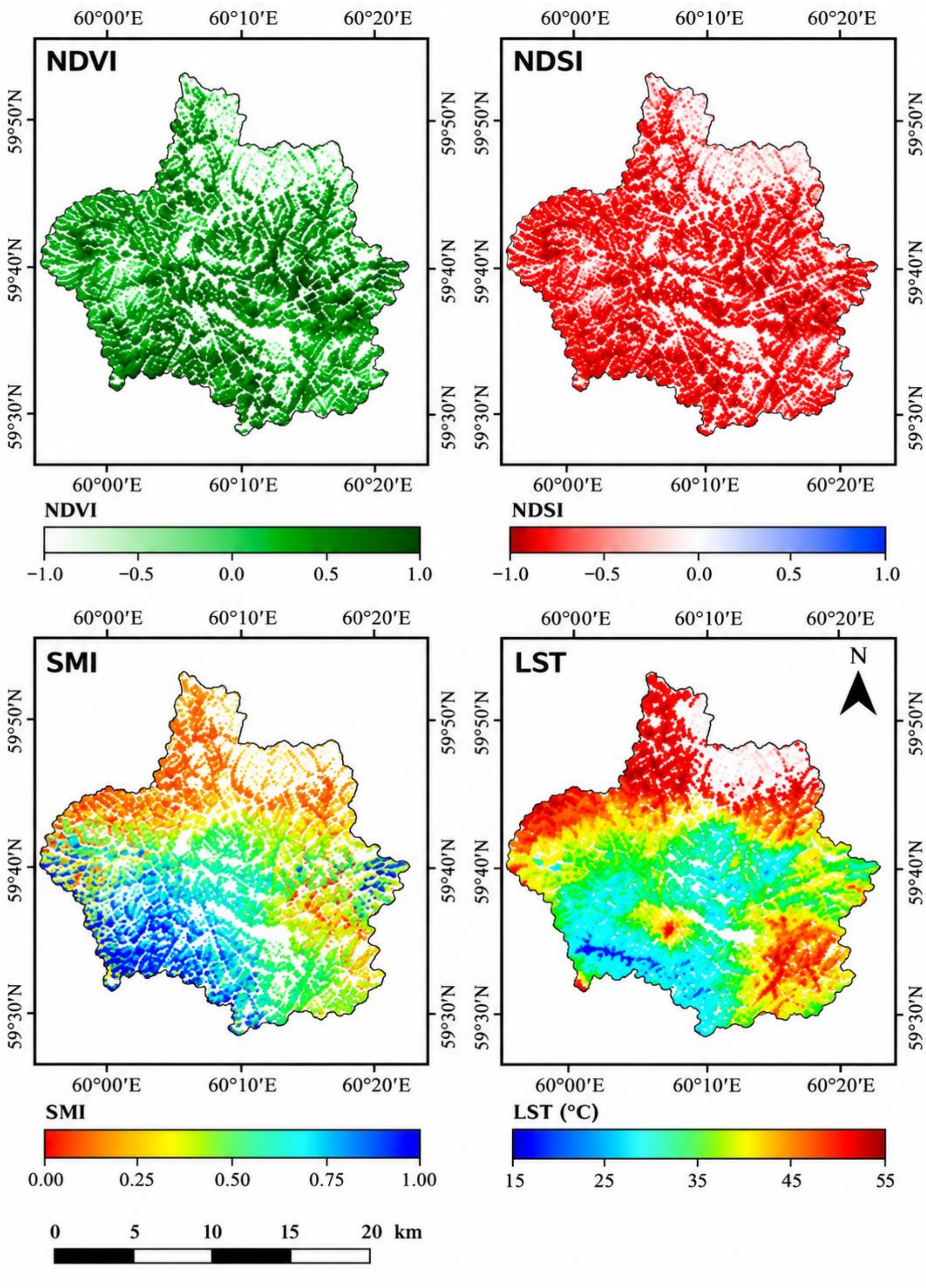

Figure 4. Spatial layers used for soil salinity modeling, including NDVI, NDSI, SMI, and LST derived from Sentinel-2 imagery.

We used the following variables to develop the models: EC (Figure 3), NDVI, NDSI, SMI (NDMI), and land surface temperature (LST) (Figure 4). The calculation of these variables is described in Table 1.

Table 1. Descriptive statistical parameters of the predictor and response variables used for SSM.

Variable name	Equation	Parameters
EC	$EC = \frac{L}{RA}$	L: Distance between electrodes R: Electrical resistance A: Cross sectional area
NDVI	$NDVI = \frac{NIR - RED}{NIR + RED}$	R: RED (665 nm) NIR: Near infrared (842 nm)
NDSI	$NDSI = \frac{R - NIR}{R + NIR}$	R: RED (665 nm) NIR: Near infrared (842 nm)
NDMI (SMI)	$NDM = \frac{NIR - SWIR1}{NIR + SWIR1}$	SWIR: Short wave infrared (1610 nm) NIR: Near infrared (842 nm)
LST	LST°C = (DN × 0.02) − 273.15	DN: pixels mean from MODIS 00.2: scale factor 273.15: K

2.6. Accuracy Assessment

To evaluate the accuracy of the models, the soil salinity collection was randomly divided into training (70%: 14 soil datasets) and testing (30%: 6 soil datasets). The accuracy of the RF, PLSR, and MLR models was measured using three reliable indicators: coefficient of determination (R^2), RMSE, and MAE. The values of the abovementioned metrics range from 0 to +1. R^2 coefficient of determination represents the statistical connection between the measured and projected values. The RMSE is the square root of the average of the proportional discrepancies among the measured and projected variables. The MAE of the model prediction is calculated from the observed data, regardless of the error direction. These statistics are shown in Equation (2) by Ma and Tashpolat (2023), Equation (3) by Fan *et al*. (2015)and Equation (4) by Hoa *et al*. (2019). where y_i signifies the measurements using an average of $\bar{y}$, $\hat{y}$ refers the projected outcomes, and N represents the total number of observations.

$$R^2 = 1 - \frac{\sum(\hat{y}_i - y_i)^2}{\sum(y_i - \bar{y}_i)^2} \tag{2}$$

$$RMSE = \sqrt{\frac{\sum(\hat{y}_i - y_i)^2}{N}} \tag{3}$$

$$MAE = \frac{1}{n}\sum_{i=1}^{n}|\hat{y}_i - y_i| \tag{4}$$

3. Results

3.1. Field Observation Data

As previously mentioned, 20 soil samples (0–30 cm) were collected from 20 representative locations across the irrigated agricultural lands of the study area, which cover an area of 758 km^2 area. A stratified spatial sampling technique was used to ensure that the sampling points accurately represented the primary agricultural areas and the existing heterogeneity in land cover and salinity conditions throughout the study area. The sampling sites were spread over the area to maximize spatial coverage while considering field accessibility and logistical restrictions. Table 2 presents soil EC measurements, together with the coordinates of the sampling locations. To facilitate the spatial analysis and visualization of salinity patterns, the measured EC values (0–7.32 dS m^{-1}) were grouped into four salinity classes based on the observed range of field measurements: non-saline (0–2.11 dS m^{-1}), slightly saline (2.11–4.27 dS m^{-1}), moderately saline (4.28–6.11 dS m^{-1}), and highly saline (6.12–7.32 dS m^{-1}). The dominant salts in the study area were sodium and chloride compounds.

Table 2. EC values measured at 20 field sampling locations across 758 km² of irrigated agricultural land in the Shimbay district, Republic of Karakalpakstan, and used for the calibration and validation of the soil salinity models.

№	Coordinates	EC	№	Coordinates	EC	№	Coordinates	EC	№	Coordinates	EC
1	43°01'38.1"N 59°57'56.7"E	4.81	6	43°10′27.5″N 59°38′39.8″E	6.73	11	42°54′06.7″N 59°37′57.6″E	6.91	16	43°08′36.1″N 59°51′29.4″E	6.81
2	43°06'26.2"N 59°50'27.7"E	4.29	7	43°07′23.1″N 59°35′12.7″E	6.52	12	42°59′22.7″N 59°56′51.6″E	7.12	17	43°04′55.8″N 59°48′22.7″E	7.15
3	43°03'15.0"N 59°34'24.5"E	2.11	8	43°01′24.3″N 59°30′48.8″E	6.91	13	42°57′56.2″N 59°35′56.7″E	7.12	18	43°01′11.9″N 59°47′36.7″E	7.32
4	42°51'29.3"N 59°45'09.1"E	1.98	9	42°49′49.2″N 59°48′43.0″E	7.32	14	43°05′41.1″N 59°30′27.4″E	6.36	19	43°01′43.1″N 59°40′27.1″E	6.94
5	42°58'09.9"N 59°48'30.5"E	6.12	10	42°55′39.8″N 59°54′17.1″E	6.2	15	43°05′54.2″N 59°39′51.3″E	6.81	20	42°58′14.7″N 59°41′31.4″E	6.91

3.2. Spatial Distribution of Salinization Data

Soil salinity dynamics were investigated using Sentinel-2 data integrated with GEE and agricultural land zones derived from ESA WorldCover (Figure 6). The NDSI for April (2017–2025) demonstrated significant interannual variability (Figure 5).

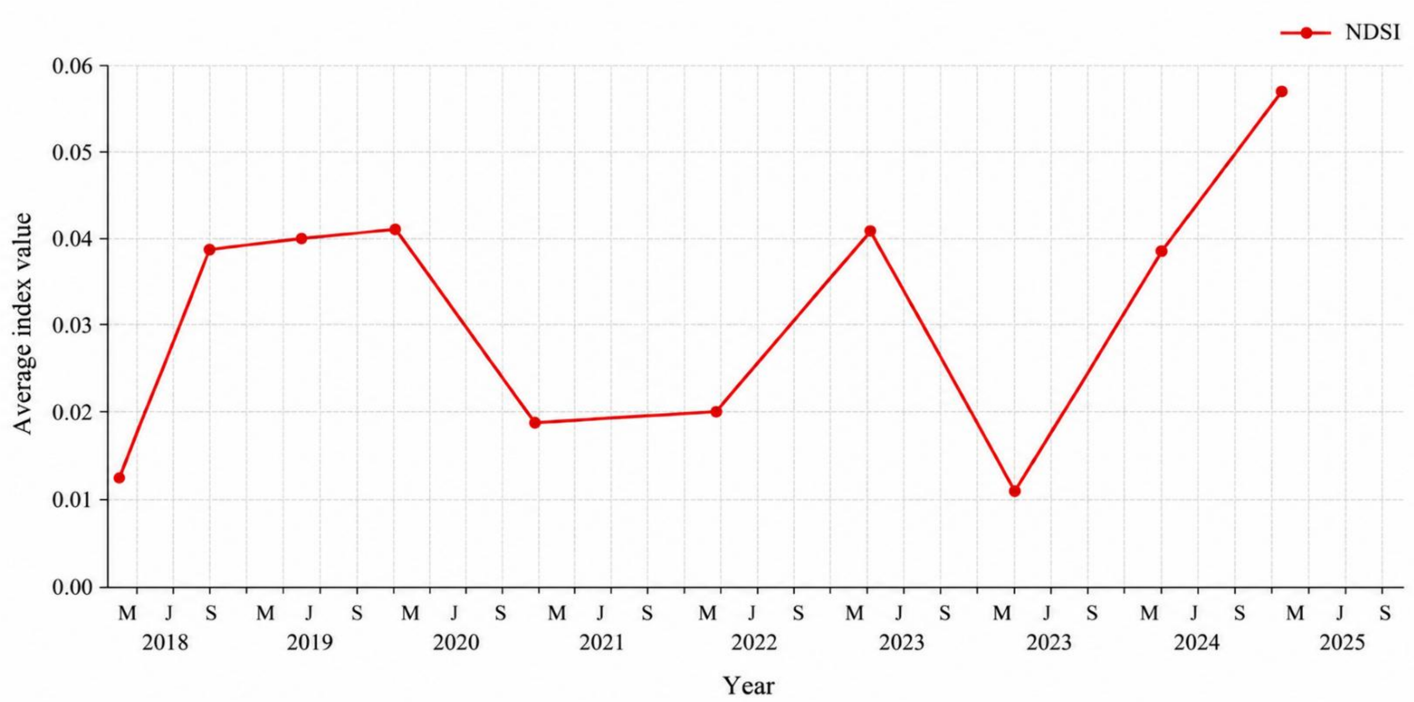

Figure 5. Temporal variation of the average NDSI across agricultural lands in the Shimbay district from 2018 to 2025, derived from Sentinel-2 imagery (10 m resolution).

From 2018 to 2025, the NDSI values ranged between 0.011 and 0.058. The salinity levels were relatively high in 2018 (0.045) and 2019 (0.041) but decreased in 2020–2021 (~0.020–0.021). Salinity increased again in 2022 (0.041), then fell drastically in 2023 (0.011), implying potential flushing or better moisture levels. A substantial increasing pattern was observed in 2024 (0.039), which peaked in 2025 (0.058), indicating increased salt accumulation.

In addition to NDSI, the temporal changes in vegetation, moisture, and heat conditions were investigated using NDVI, SMI, and LST (Table 3). The NDVI values varied from 0.417 to 0.536, with the highest value recorded in 2017 (0.536), followed by a general decline and stabilization at 0.43–0.49 from 2018 to 2025, showing moderate and relatively stable vegetative state conditions. The SMI results were continuously negative (ranging from −0.007 to −0.059), indicating dry soil conditions throughout the research period. The lowest moisture values were recorded in 2025 (−0.059) and 2018–2019 (−0.047), indicating growing soil dryness. The LST fluctuated from 26.7°C in 2018 to 32.98°C in 2022, then decreased slightly but remained relatively high (~30–31°C) during 2023–2025. Elevated LST values coincide with lower soil moisture levels and may contribute to increased evaporation and salt accumulation.

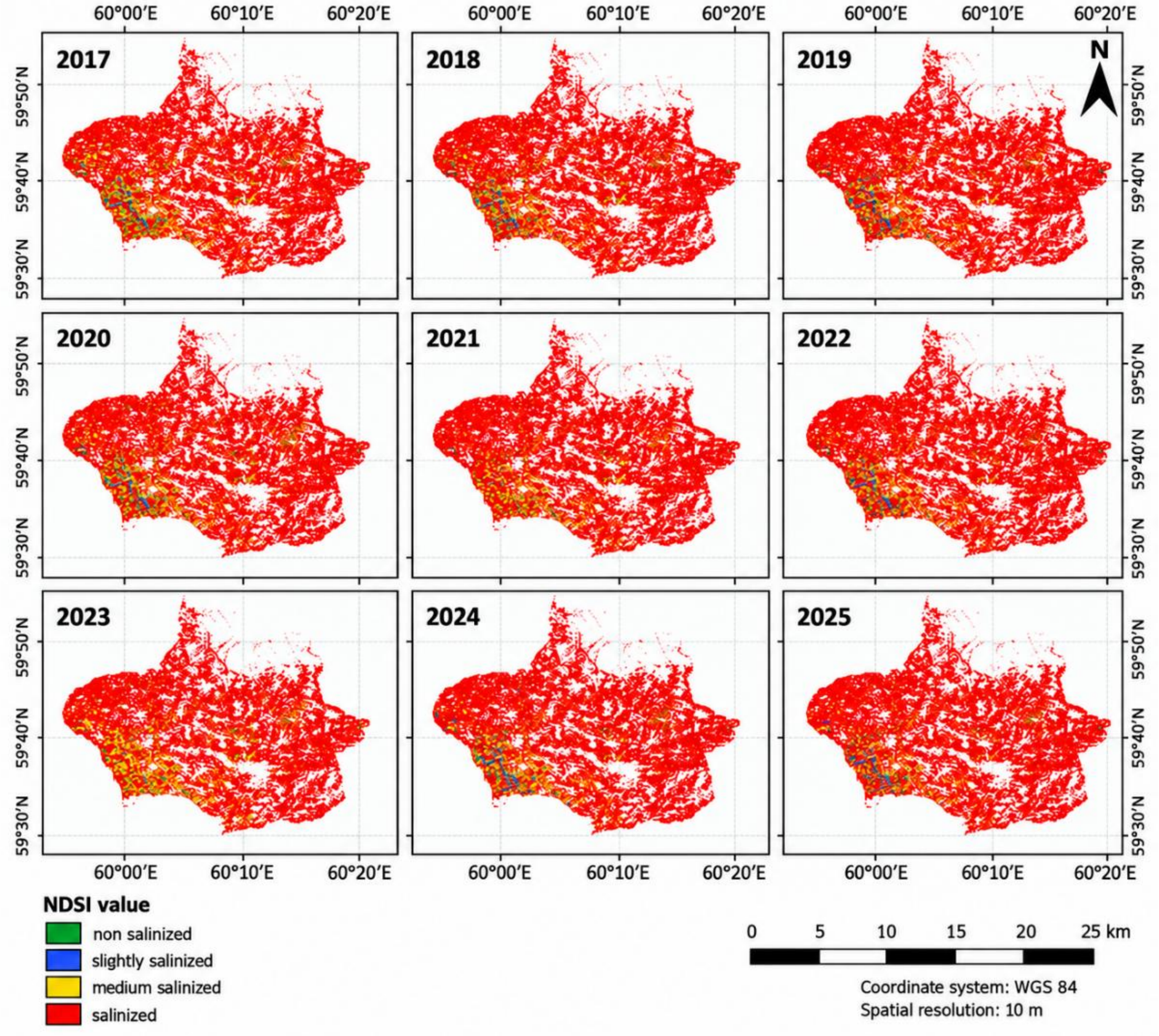

Figure 6. Spatial distribution of soil salinity across agricultural lands in the Shimbay district, derived from Sentinel-2 imagery (10 m spatial resolution).

Table 3. Temporal variation of the average NDVI, SMI, and LST values across agricultural lands in the Shimbay district from 2018 to 2025

Index	2017	2018	2019	2020	2021	2022	2023	2024	2025
NDVI	0.536	0.417	0.494	0.477	0.43	0.432	0.425	0.436	0.434
SMI	−0.007	−0.047	−0.047	−0.02	−0.019	−0.042	−0.018	−0.044	−0.059
LST	27.9	26.6	29.0	28.3	30.9	32.9	31.4	30.9	30.7

3.3. Modeling of Soil Salinity Assessment

The PLSR model was adopted in GEE to estimate soil salinity (EC), with NDVI, NDSI, and SMI as predictor parameters. A Sentinel-2 composite for April 2025 was used to obtain spectral data at sampling points. The model was developed with two latent factors (LV2) to account for multi-collinearity and record the highest correlation between predictors and EC.

PLSR was implemented using two latent variables (LV1 and LV2). The two-component model was adopted to reduce the predictor variables' dimensionality while preserving the main covariance structure between the Sentinel-2 spectral indices (NDVI, NDSI, and SMI) and soil EC. The model performance was evaluated using R^2, RMSE, and MAE. No cross-validation procedure was applied during latent variable selection; therefore, future studies should investigate the optimal number of latent variables using k-fold or leave-one-out cross-validation.

The model accurately predicted soil salinity, accounting for more than 93% of the variability ($R^2 = 0.934$). The error statistics were relatively low, with RMSE = 0.398 and MAE = 0.329, indicating that the predictions were highly accurate and reliable (Figure 7).

The calculated Variable Importance in Projection scores emphasized each predictor's contribution, indicating that spectral indices associated with salinity and moisture play an important role in understanding EC variability. The spatial implementation of the model produced an ongoing salinity map that successfully described the variation of soil salinity throughout agricultural fields.

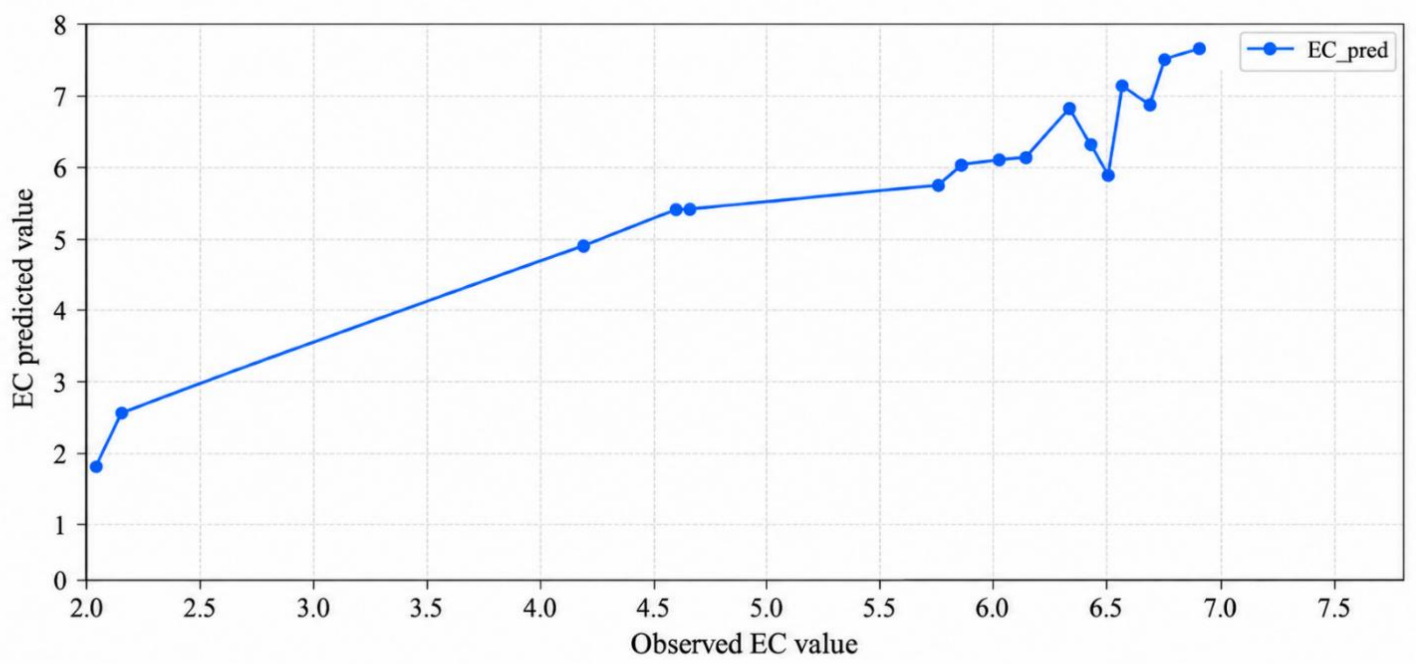

Figure 7. Performance of the PLSR model for soil salinity estimation using Sentinel-2-derived spectral indices

The RF regression model was used to measure soil salinity (EC), with spectral indices (NDVI, NDSI, SMI) and LST as predictor parameters. The input features were derived using a multi-temporal Sentinel-2 composite (April-June 2025), with the study focusing on agricultural lands. The model accurately predicted EC with a coefficient of determination of $R^2 = 0.810$, explaining 81% of the variability. The error metrics were greater than those of the PLSR model, with RMSE = 0.966 and MAE = 0.728, indicating modest prediction accuracy (Figure 8).

Feature importance analysis revealed that salinity- and moisture-related indices (NDSI and SMI) and temperature (LST) contributed the most to the model, with NDVI playing a secondary role. The RF model successfully captured non-linear interactions between predictors and EC, allowing us to create a spatially continuous salinity map that captured the heterogeneity of the research area.

RF regression was implemented in GEE using the Smile RF algorithm. To ensure reproducibility, the model was developed with 20 decision trees (number of trees = 20) and a fixed random seed of 42. The predictor variables included NDVI, NDSI, SMI, and LST, which were extracted from the Sentinel-2 median composite. No additional feature selection procedure was applied; instead, all predictor variables were included in the development of the model. The relative importance of each predictor was evaluated using the built-in feature importance function (trained.explain()), which quantifies each variable's contribution to the prediction model. The model performance was assessed using the coefficient of determination (R^2), RMSE, and MAE.

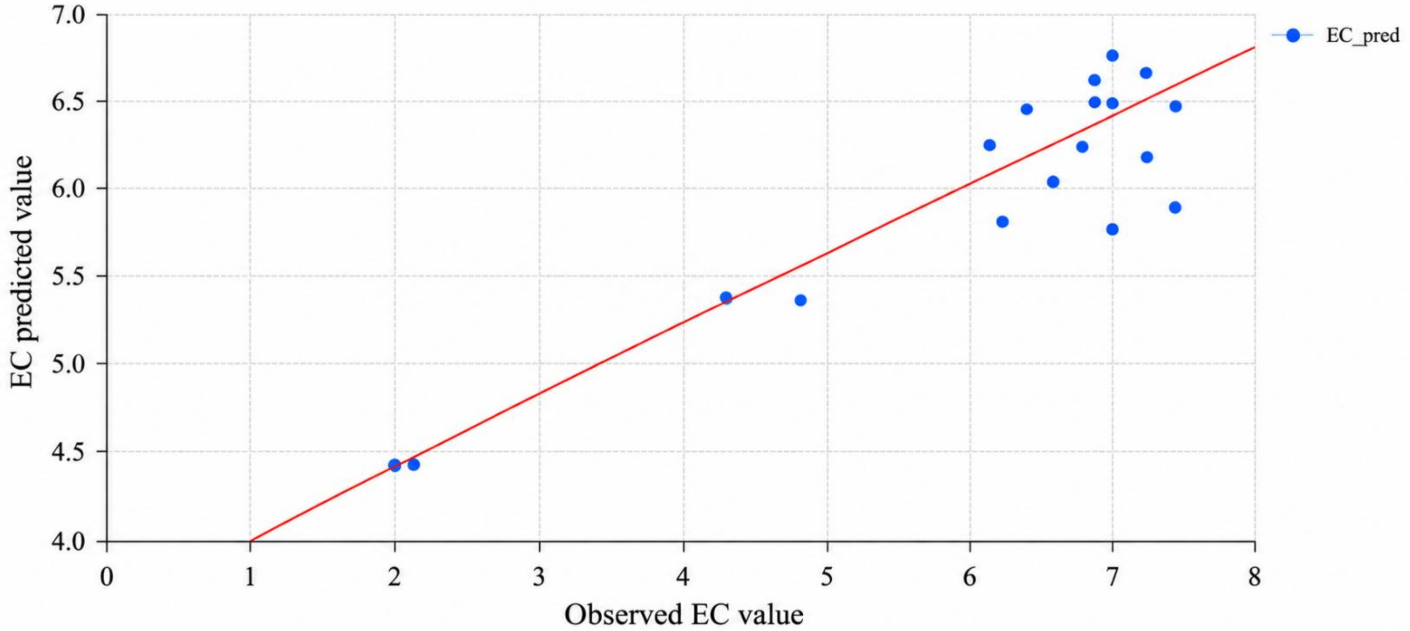

Figure 8. Performance of the RF model for soil salinity estimation using Sentinel-2-derived spectral indices.

The soil salinity (EC) was estimated using the MLR model, with NDVI, NDSI, and SMI as predictor variables collected from Sentinel-2 data. The model showed a linear link between spectral indices and EC values using field observations. MLR was implemented in GEE using NDVI, NDSI, and SMI as predictor variables and soil EC as the response variable. The regression coefficients were estimated using the ee.Reducer.linearRegression() function, and the resulting equation was used to predict soil salinity. The model performance was evaluated using the coefficient of determination (R^2), RMSE, and MAE. Because the GEE linear regression implementation does not provide statistical inference for regression coefficients, their statistical significance (e.g., p-values and confidence intervals) was not evaluated in this study.

The MLR model had moderate predictive accuracy ($R^2 = 0.677$), explaining approximately 67.7% of the EC variability. The error metrics were RMSE = 0.902 and MAE = 0.687, indicating a reasonable but lower accuracy than the more advanced techniques (Figure 9). The MLR model has limitations in describing complicated and non-linear connections between environmental factors and soil salinity despite its straightforward nature and ease of comprehension. Consequently, its prediction ability is lower than that of the PLSR and RF models.

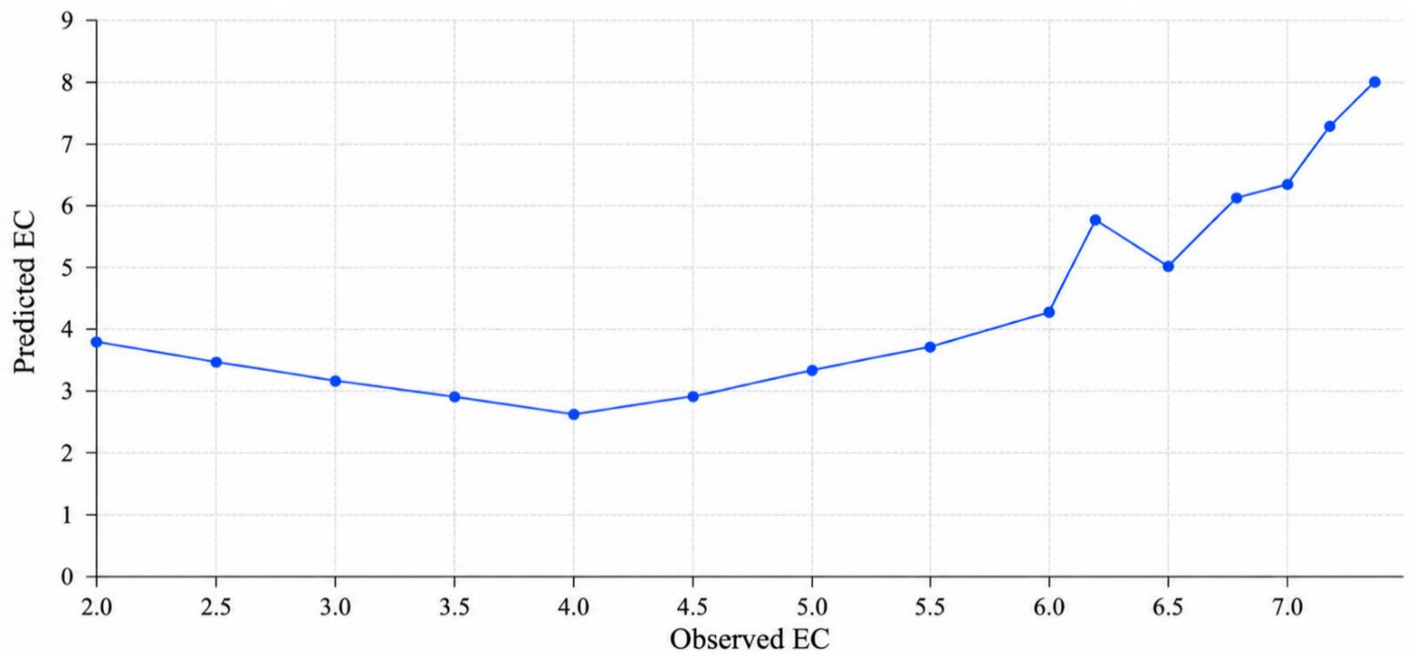

Figure 9. Performance of the MLR model for soil salinity estimation using Sentinel-2-derived spectral indices.

4. Discussion

4.1. Performance of the Machine Learning and Regression Models

The PLSR model has the highest prediction accuracy (R^2 = 0.934), surpassing RF; R^2 = 0.810) and MLR; R^2 = 0.677). The higher PLSR performance suggests that dimensionality reduction and latent variable extraction were efficient in capturing the correlations between Sentinel-2 spectral information and soil salinity. The ability of PLSR to manage multicollinearity among spectral bands and salinity-related variables makes it ideal for remote sensing applications in which predictor variables are frequently highly correlated. Kaplan *et al*. (2023) found that Sentinel-2-based regression and ML models can effectively forecast soil salinity in arid areas.

Although RF gave reliable predictions, its accuracy was lower than that of PLSR. This discrepancy could be attributed to the small number of field samples and the spectral features of the research area, where linear latent structures were more informative than complicated non-linear interactions. Previous research has demonstrated that RF performs best with large training datasets and highly varied environmental circumstances (Aksoy *et al*., 2022; Sulieman *et al*., 2023). Xiao *et al*. (2024) found that combining optical and radar data significantly enhanced RF-based salinity prediction in arid agricultural areas.

The poor MLR performance implies that simple linear connections are insufficient to capture the complex interplay between spectral features and soil salinity in irrigated agricultural situations. These findings confirm earlier studies indicating that advanced regression and ML approaches routinely outperform standard statistical methods for soil salinity mapping (Kaplan, 2025; Wang *et al*., 2024). The findings emphasize the significance of adopting modeling methodologies capable of capturing complicated connections among RS variables.

Sentinel-2 spectral bands and salinity-related metrics were applied to enhance the spatial assessment of soil salinity across the study area. Vegetation- and moisture-related indices, such as NDVI, NDSI, and SMI, were strongly associated with field-measured EC, implying that the vegetation state, soil moisture, and surface features are all intimately related to salinity dynamics. The excellent spatial resolution, frequent revisit time, and free availability of Sentinel-2 imagery make it a valuable data source for operational soil salinity monitoring and sustainable agriculture management in arid locations.

4.2. Implications for Sustainable Land Management in Karakalpakstan

Soil salinization is a major ecological and agricultural concern in the Republic of Karakalpakstan. It is caused by arid climatic conditions, irrigation techniques, shallow groundwater, and the long-term environmental effects of the Aral Sea disaster. Thus, spatial identification and monitoring of salinity-affected agricultural land are critical for better irrigation management, crop productivity, land restoration, and climate adaptation strategies.

The findings indicate that combining remote sensing spectral indicators with regression and ML approaches provides an accurate and feasible framework for assessing regional soil salinity. Compared with traditional field sampling, the combination of Sentinel-2 images with statistical and ML models allows for faster, more cost-effective, and spatially consistent monitoring of large agricultural areas. Recent research has revealed similar results, emphasizing the expanding relevance of remote sensing and ML in enabling sustainable agricultural and environmental monitoring in dry settings (Kaplan, 2025).

Among the models tested, PLSR had the best predictive performance, demonstrating that multispectral satellite data can successfully support precision agriculture and long-term land management in ecologically critical areas. The resulting salinity maps can assist agricultural authorities, environmental agencies, and land managers in identifying priority locations for salinity mitigation, irrigation planning, and soil restoration. Furthermore, these geographical datasets help improve the evaluation of land suitability and promote sustainable agricultural growth throughout the Aral Sea Basin.

The application of remote sensing-based salinity evaluation is especially critical in Karakalpakstan, where extreme climate, limited water resources, and secondary salinization continue to endanger agricultural production and food security. Previous research in Uzbekistan has also emphasized the importance of satellite-based salinity monitoring for irrigated agricultural systems in dry areas (Ivushkin *et al*., 2017). Similarly, adaptive salinity assessment systems have been advocated to promote responsive land management under changing climatic conditions (Mirzaee *et al*., 2024; Wang *et al*., 2024).

4.3. Study Limitations

Despite the encouraging results, several limitations should be acknowledged. First, the developed models were calibrated and validated using field observations collected from only 20 sampling locations, which may limit their robustness and generalizability to larger or more heterogeneous agricultural areas. In addition, model validation was based on a single 70/30 train-test split, which may increase the uncertainty of the reported performance metrics compared with k-fold cross-validation or leave-one-out cross-validation. Second, the analysis relied primarily on Sentinel-2 optical imagery, which is affected by cloud cover and cannot directly capture SSU conditions. Third, the modeling framework was developed specifically for the environmental and agricultural conditions of the Chimbay district; therefore, local calibration and validation should precede its application to other arid regions. Finally, although the PLSR model demonstrated high predictive accuracy, additional field observations, multi-season datasets, and the integration of complementary remote sensing data (e.g., SAR or hyperspectral imagery) could further improve model robustness and transferability. Future research should also employ more comprehensive validation strategies, such as k-fold cross-validation or bootstrapping, together with larger field datasets to provide more reliable estimates of model performance across different environmental conditions.

5. Conclusion

This study demonstrated the efficacy of using remote sensing data and modeling tools to estimate soil salinity dynamics in the dry Shimbay district of Karakalpakstan. The multi-temporal examination of Sentinel-2 data indicated significant interannual fluctuations in soil salinity, with NDSI values ranging from 0.011 to 0.058 between 2018 and 2025. The findings revealed a general upward trend in salinization in recent years, particularly in 2024-2025, indicating increased salt accumulation.

Environmental parameters revealed that moisture deficiency and temperature conditions had a significant influence on soil salinity. Consistently negative SMI measurements revealed chronic soil dryness, whereas elevated LST values (up to 32.9°C) increased evaporation and salt concentrations. Despite increased salinity stress, vegetation conditions, as measured by NDVI, remained relatively steady, indicating moderate crop cover. Among the evaluated models, PLSR achieved the highest predictive performance (R^2 = 0.934, RMSE = 0.398, MAE = 0.329), followed by RF (R^2 = 0.810, RMSE = 0.966, MAE = 0.728) and MLR (R^2 = 0.677, RMSE = 0.902, MAE = 0.687). These findings suggest that PLSR is well suited for modeling soil salinity under the study area's environmental conditions.

Although the proposed approach showed strong predictive performance, the results should be interpreted in light of the study's limitations, including the limited number of field samples, the reliance on Sentinel-2 optical imagery, the use of a single 70/30 train-test split for model validation, the absence of uncertainty analysis, and the focus on a single study area. Consequently, further validation using larger datasets, more rigorous validation strategies (e.g., k-fold cross-validation), uncertainty assessment, multi-season observations, and different agro-ecological regions is required before broader application.

The findings highlight the potential of combining satellite-derived indices with advanced modeling techniques to support the assessment of regional soil salinity and sustainable land management in arid environments. Future research should incorporate additional environmental variables, expand spatial and temporal coverage, and evaluate model performance under diverse climatic and agricultural conditions.

Acknowledgements

The authors would like to thank the anonymous reviewers for their valuable comments and constructive suggestions, which have significantly improved the quality of this manuscript. Also, the authors thank Enago (www.enago.com) for the English language review.

Author Contributions

Conceptualization: Abdikairov B, Juliev M; methodology: Abdikairov B, Kholmurodova M; **investigation:** Turdaliev S, Khadjieva Z, Djanpulatova Z; **writing—original draft preparation:** Abdikairov B, Juliev M; **writing—review and editing:** Abdikairov B, Juliev M ; **visualization:** Kholmurodova M, Djanpulatova G. All authors have read and agreed to the published version of the manuscript.

Conflict of interest

Authors declare that they have no conflict of interest.

Data availability

The author confirms that all data generated or analyzed during the study are included in this article.

Funding

The research received no external funding.

References

Abdikairov, B., Juliev, M., & Kholmurodova, M. (2024). Analyses and assessment of soil salinity modeling: Review of papers from Scopus database. *Journal of Geology, Geography and Geoecology*, *33*(4), 647–661. https://doi.org/10.15421/112459

Abou Samra, R. M., & Ali, R. R. (2018). The development of an overlay model to predict soil salinity risks by using remote sensing and GIS techniques: A case study in soils around Idku Lake, Egypt. *Environmental Monitoring and Assessment*, *190*(12). Scopus. https://doi.org/10.1007/s10661-018-7079-3

Aihaiti, A., Nurmemet, I., Yu, X., Aili, Y., Li, S., Lv, X., & Qin, Y. (2025). An enhanced soil salinity estimation method for arid regions using multisource remote sensing data and advanced feature selection. *CATENA*, *256*, 109116. https://doi.org/10.1016/j.catena.2025.109116

Aksoy, S., Yildirim, A., Gorji, T., Hamzehpour, N., Tanik, A., & Sertel, E. (2022). Assessing the performance of machine learning algorithms for soil salinity mapping in Google Earth Engine platform using Sentinel-2A and Landsat-8 OLI data. *Advances in Space Research*, *69*(2), 1072–1086. https://doi.org/10.1016/j.asr.2021.10.024

Allbed, A., Kumar, L., & Aldakheel, Y. Y. (2014). Assessing soil salinity using soil salinity and vegetation indices derived from IKONOS high-spatial resolution imageries: Applications in a date palm dominated region. *Geoderma*, *230–231*, 1–8. https://doi.org/10.1016/j.geoderma.2014.03.025

Amir Latif, R. M., Arshad, A., He, J., Habib Ur-Rahman, M., Mansour, F., Sabagh, A. E., & Al-Ashkar, I. (2025). Integrating machine learning with multitemporal remote sensing to quantify spatial soil salinity. *The Egyptian Journal of Remote Sensing and Space Sciences*, *28*(3), 573–586. https://doi.org/10.1016/j.ejrs.2025.08.005

Avdan, U., Kaplan, G., Küçük Matcı, D., Yiğit Avdan, Z., Erdem, F., Tuğba Mızık, E., & Demirtaş, İ. (2022). Soil salinity prediction models constructed by different remote sensors. *Physics and Chemistry of the Earth*, *128*. Scopus. https://doi.org/10.1016/j.pce.2022.103230

Corwin, D. L., Rhoades, J. D., & Šimůnek, J. (2007). Leaching requirement for soil salinity control: Steady-state versus transient models. *Agricultural Water Management*, *90*(3), 165–180. Scopus. https://doi.org/10.1016/j.agwat.2007.02.007

Das, A., Bhattacharya, B. K., Setia, R., Jayasree, G., & Sankar Das, B. (2023). A novel method for detecting soil salinity using AVIRIS-NG imaging spectroscopy and ensemble machine learning. *ISPRS Journal of Photogrammetry and Remote Sensing*, *200*, 191–212. https://doi.org/10.1016/j.isprsjprs.2023.04.018

Djanibekov, U., & Finger, R. (2018). Agricultural risks and farm land consolidation process in transition countries: The case of cotton production in Uzbekistan. *Agricultural Systems*, *164*, 223–235. https://doi.org/10.1016/j.agsy.2018.03.009

Duan, Z., Wang, X., & Sun, L. (2022). Monitoring and Mapping of Soil Salinity on the Exposed Seabed of the Aral Sea, Central Asia. *Water*, *14*(9), 1438. https://doi.org/10.3390/w14091438

Dubovyk, O., Menz, G., Conrad, C., Kan, E., Machwitz, M., & Khamzina, A. (2013). Spatio-temporal analyses of cropland degradation in the irrigated lowlands of Uzbekistan using remote-sensing and logistic regression modeling. *Environmental Monitoring and Assessment*, *185*(6), 4775–4790. https://doi.org/10.1007/s10661-012-2904-6

Etesami, H., & Noori, F. (2019). Soil Salinity as a Challenge for Sustainable Agriculture and Bacterial-Mediated Alleviation of Salinity Stress in Crop Plants. In M. Kumar, H. Etesami, & V. Kumar (Eds.), *Saline Soil-based Agriculture by Halotolerant Microorganisms* (pp. 1–22). Springer Singapore. https://doi.org/10.1007/978-981-13-8335-9_1

Fan, X., Liu, Y., Tao, J., & Weng, Y. (2015). Soil Salinity Retrieval from Advanced Multi-Spectral Sensor with Partial Least Square Regression. *Remote Sensing*, *7*(1), 488–511. https://doi.org/10.3390/rs70100488

Farahmand, N., & Sadeghi, V. (2020). Estimating Soil Salinity in the Dried Lake Bed of Urmia Lake Using Optical Sentinel-2 Images and Nonlinear Regression Models. *Journal of the Indian Society of Remote Sensing*, *48*(4), 675–687. Scopus. https://doi.org/10.1007/s12524-019-01100-8

Golestani, M., Mosleh Ghahfarokhi, Z., Esfandiarpour-Boroujeni, I., & Shirani, H. (2023). Evaluating the spatiotemporal variations of soil salinity in Sirjan Playa, Iran using Sentinel-2A and Landsat-8 OLI imagery. *CATENA*, *231*, 107375. https://doi.org/10.1016/j.catena.2023.107375

Hoa, P. V., Giang, N. V., Binh, N. A., Hai, L. V. H., Pham, T.-D., Hasanlou, M., & Tien Bui, D. (2019). Soil Salinity Mapping Using SAR Sentinel-1 Data and Advanced Machine Learning Algorithms: A Case Study at Ben Tre Province of the Mekong River Delta (Vietnam). *Remote Sensing*, *11*(2), 128. https://doi.org/10.3390/rs11020128

Ibrakhimov, M., Awanb, U. K., International Center for Agricultural Research in Dry Areas, Sultanov, M., Khorezm Rural Advisory Support Service, Akramkhanov, A., International Center for Agricultural Research in Dry Areas, Djumaboev, K., International Water Management Institute, Conrad, C., University of Würzburg Institute of Geography and Geology, Lamers, J., & Center for Development Research. (2020). Combining remote sensing and modeling approaches to assess soil salinity in irrigated areas of the Aral Sea Basin. *Central Asian Journal of Water Research*, *5*(2), 64–81. https://doi.org/10.29258/CAJWR/2019-R1.v5-2/64-81eng

Ivushkin, K., Bartholomeus, H., Bregt, A. K., & Pulatov, A. (2017). Satellite Thermography for Soil Salinity Assessment of Cropped Areas in Uzbekistan. *Land Degradation & Development*, *28*(3), 870–877. https://doi.org/10.1002/ldr.2670

Ivushkin, K., Bartholomeus, H., Bregt, A. K., Pulatov, A., Kempen, B., & De Sousa, L. (2019). Global mapping of soil salinity change. *Remote Sensing of Environment*, *231*, 111260. https://doi.org/10.1016/j.rse.2019.111260

Jia, P., He, W., Hu, Y., Liang, Y., Liang, Y., Xue, L., Zamanian, K., & Zhao, X. (2024). Inversion of coastal cultivated soil salt content based on multi-source spectra and environmental variables. *Soil and Tillage Research*, *241*, 106124. https://doi.org/10.1016/j.still.2024.106124

Jumaniyazov, I., Juliev, M., Khudaybergenov, Y., Jaksibaev, R., Orazbaev, A., & Amangeldieva, U. (2024). Analysis of soil salinity monitoring in irrigated areas (in case of Shimbay district, Republic of Karakalpakstan). *E3S Web of Conferences*, *590*, 01007. https://doi.org/10.1051/e3sconf/202459001007

Jumaniyazov, I., Juliev, M., Reimov, M., Oymatov, R., Inamov, A., Yunusov, B., & Abdramanova, D. (2026). Assessing Spatiotemporal Dynamics of AI-based Land Use and Land Cover through Sentinel-2 Time-Series Imagery: A Case Study of the Shimbay District, Republic of Karakalpakstan, Uzbekistan. *Forum Geografi*, *40*(1), 44–56. https://doi.org/10.23917/forgeo.8724

Kaplan. (2025). *Detection of Soil Salinity Using Remote Sensing and Machine Learning: Innovative Approaches and Contributions*. https://doi.org/10.5281/ZENODO.15094133

Kaplan, G., Gašparović, M., Alqasemi, A. S., Aldhaheri, A., Abuelgasim, A., & Ibrahim, M. (2023). Soil salinity prediction using Machine Learning and Sentinel – 2 Remote Sensing Data in Hyper – Arid areas. *Physics and Chemistry of the Earth, Parts A/B/C*, *130*, 103400. https://doi.org/10.1016/j.pce.2023.103400

Khongnawang, T., Zare, E., Srihabun, P., Khunthong, I., & Triantafilis, J. (2022). Digital soil mapping of soil salinity using EM38 and quasi-3d modelling software (EM4Soil). *Soil Use Manage.*, *38*(1), 277–291. Scopus. https://doi.org/10.1111/sum.12778

Ma, L., Ma, F., Li, J., Gu, Q., Yang, S., Wu, D., Feng, J., & Ding, J. (2017). Characterizing and modeling regional-scale variations in soil salinity in the arid oasis of Tarim Basin, China. *Geoderma*, *305*, 1–11. Scopus. https://doi.org/10.1016/j.geoderma.2017.05.016

Ma, Y., & Tashpolat, N. (2023). Remote Sensing Monitoring of Soil Salinity in Weigan River–Kuqa River Delta Oasis Based on Two-Dimensional Feature Space. *Water*, *15*(9), 1694. https://doi.org/10.3390/w15091694

Micklin, P. (2007). The Aral Sea Disaster. *Annual Review of Earth and Planetary Sciences*, *35*(1), 47–72. https://doi.org/10.1146/annurev.earth.35.031306.140120

Mirzaee, S., Nafchi, A. M., Ostovari, Y., Seifi, M., Ghorbani-Dashtaki, S., Khodaverdiloo, H., Chakherlou, S., Taghizadeh-Mehrjardi, R., & Raei, B. (2024). Monitoring and assessment of spatiotemporal soil salinization in the Lake Urmia region. *Environmental Monitoring and Assessment*, *196*(10), 958. https://doi.org/10.1007/s10661-024-13055-6

Mohamed, S. A., Metwaly, M. M., Metwalli, M. R., AbdelRahman, M. A. E., & Badreldin, N. (2023). Integrating Active and Passive Remote Sensing Data for Mapping Soil Salinity Using Machine Learning and Feature Selection Approaches in Arid Regions. *Remote Sensing*, *15*(7), 1751. https://doi.org/10.3390/rs15071751

Muhetaer, N., Nurmemet, I., Abulaiti, A., Xiao, S., & Zhao, J. (2022). An Efficient Approach for Inverting the Soil Salinity in Keriya Oasis, Northwestern China, Based on the Optical-Radar Feature-Space Model. *Sensors*, *22*(19). Scopus. https://doi.org/10.3390/s22197226

Nawar, S., Buddenbaum, H., Hill, J., & Kozak, J. (2014). Modeling and mapping of soil salinity with reflectance spectroscopy and landsat data using two quantitative methods (PLSR and MARS). *Remote Sensing*, *6*(11), 10813–10834. Scopus. https://doi.org/10.3390/rs61110813

Ngabire, M., Wang, T., Xue, X., Liao, J., Sahbeni, G., Huang, C., Duan, H., & Song, X. (2022). Soil salinization mapping across different sandy land-cover types in the Shiyang River Basin: A remote sensing and multiple linear regression approach. *Remote Sensing Applications: Society and Environment*, *28*, 100847. https://doi.org/10.1016/j.rsase.2022.100847

Nurmemet, I., Sagan, V., Ding, J.-L., Halik, Ü., Abliz, A., & Yakup, Z. (2018). A WFS-SVM model for soil salinity mapping in Keriya Oasis, Northwestern China using polarimetric decomposition and fully PolSAR data. *Remote Sensing*, *10*(4). Scopus. https://doi.org/10.3390/rs10040598

Qadir, M., Quillérou, E., Nangia, V., Murtaza, G., Singh, M., Thomas, R. J., Drechsel, P., & Noble, A. D. (2014). Economics of salt-induced land degradation and restoration. *Natural Resources Forum*, *38*(4), 282–295. https://doi.org/10.1111/1477-8947.12054

Rengasamy, P. (2010). Soil processes affecting crop production in salt-affected soils. *Functional Plant Biology*, *37*(7), 613–620. https://doi.org/10.1071/FP09249

Sahbeni, G. (2021). A PLSR model to predict soil salinity using Sentinel-2 MSI data. *Open Geosciences*, *13*(1), 977–987. Scopus. https://doi.org/10.1515/geo-2020-0286

Sarkar, S. K., Rudra, R. R., Sohan, A. R., Das, P. C., Ekram, K. M. M., Talukdar, S., Rahman, A., Alam, E., Islam, M. K., & Islam, A. R. Md. T. (2023). Coupling of machine learning and remote sensing for soil salinity mapping in coastal area of Bangladesh. *Scientific Reports*, *13*(1), 17056. https://doi.org/10.1038/s41598-023-44132-4

Shahabi, M., Jafarzadeh, A. A., Neyshabouri, M. R., Ghorbani, M. A., & Valizadeh Kamran, K. (2017). Spatial modeling of soil salinity using multiple linear regression, ordinary kriging and artificial neural network methods. *Archives of Agronomy and Soil Science*, *63*(2), 151–160. https://doi.org/10.1080/03650340.2016.1193162

Shi, P., Six, J., Sila, A., Vanlauwe, B., & Van Oost, K. (2022). Towards spatially continuous mapping of soil organic carbon in croplands using multitemporal Sentinel-2 remote sensing. *ISPRS Journal of Photogrammetry and Remote Sensing*, *193*, 187–199. https://doi.org/10.1016/j.isprsjprs.2022.09.013

Shrivastava, P., & Kumar, R. (2015). Soil salinity: A serious environmental issue and plant grAowth promoting bacteria as one of the tools for its alleviation. *Saudi Journal of Biological Sciences*, *22*(2), 123–131. https://doi.org/10.1016/j.sjbs.2014.12.001

Sulieman, M. M., Kaya, F., Elsheikh, M. A., Başayiğit, L., & Francaviglia, R. (2023). Application of Machine Learning Algorithms for Digital Mapping of Soil Salinity Levels and Assessing Their Spatial Transferability in Arid Regions. *Land*, *12*(9), 1680. https://doi.org/10.3390/land12091680

Taghadosi, M. M., Hasanlou, M., & Eftekhari, K. (2019a). Retrieval of soil salinity from Sentinel-2 multispectral imagery. *European Journal of Remote Sensing*, *52*(1), 138–154. https://doi.org/10.1080/22797254.2019.1571870

Taghadosi, M. M., Hasanlou, M., & Eftekhari, K. (2019b). Soil salinity mapping using dual-polarized SAR Sentinel-1 imagery. *International Journal of Remote Sensing*, *40*(1), 237–252. https://doi.org/10.1080/01431161.2018.1512767

Taghizadeh-Mehrjardi, R., Hamzehpour, N., Hassanzadeh, M., Heung, B., Ghebleh Goydaragh, M., Schmidt, K., & Scholten, T. (2021). Enhancing the accuracy of machine learning models using the super learner technique in digital soil mapping. *Geoderma*, *399*, 115108. https://doi.org/10.1016/j.geoderma.2021.115108

Thangarasu, T., Mengash, H. A., Allafi, R., & Mahgoub, H. (2025). Spatial prediction of soil salinity: Remote sensing and machine learning approach. *Journal of South American Earth Sciences*, *156*, 105440. https://doi.org/10.1016/j.jsames.2025.105440

Wang, Han, L., Liu, L., Bai, C., Ao, J., Hu, H., Li, R., Li, X., Guo, X., & Wei, Y. (2024). Advancements and Perspective in the Quantitative Assessment of Soil Salinity Utilizing Remote Sensing and Machine Learning Algorithms: A Review. *Remote Sensing*, *16*(24), 4812. https://doi.org/10.3390/rs16244812

Wang, J., Peng, J., Li, H., Yin, C., Liu, W., Wang, T., & Zhang, H. (2021). Soil Salinity Mapping Using Machine Learning Algorithams with the Sentinel-2 MSI in Arid Areas, China. *Remote Sensing*, *13*(2), 305. https://doi.org/10.3390/rs13020305

Wang, J., Yang, T., Zhu, K., Shao, C., Zhu, W., Hou, G., & Sun, Z. (2023). A novel retrieval model for soil salinity from CYGNSS: Algorithm and test in the Yellow River Delta. *Geoderma*, *432*. Scopus. https://doi.org/10.1016/j.geoderma.2023.116417

Wang, N., Chen, S., Huang, J., Frappart, F., Taghizadeh, R., Zhang, X., Wigneron, J.-P., Xue, J., Xiao, Y., Peng, J., & Shi, Z. (2024). Global Soil Salinity Estimation at 10 m Using Multi-Source Remote Sensing. *Journal of Remote Sensing*, *4*, 0130. https://doi.org/10.34133/remotesensing.0130

Wang, Y., Xie, M., Hu, B., Jiang, Q., Shi, Z., He, Y., & Peng, J. (2022). Desert Soil Salinity Inversion Models Based on Field In Situ Spectroscopy in Southern Xinjiang, China. *Remote Sensing*, *14*(19). Scopus. https://doi.org/10.3390/rs14194962

Wang, Z., Zhang, F., Zhang, X., Chan, N. W., Kung, H., Ariken, M., Zhou, X., & Wang, Y. (2021). Regional suitability prediction of soil salinization based on remote-sensing derivatives and optimal spectral index. *Science of The Total Environment*, *775*, 145807. https://doi.org/10.1016/j.scitotenv.2021.145807

Xiao, S., Nurmemet, I., & Zhao, J. (2024). Soil salinity estimation based on machine learning using the GF-3 radar and Landsat-8 data in the Keriya Oasis, Southern Xinjiang, China. *Plant and Soil*, *498*(1–2), 451–469. https://doi.org/10.1007/s11104-023-06446-0

Zanaga, D., Van De Kerchove, R., De Keersmaecker, W., Souverijns, N., Brockmann, C., Quast, R., Wevers, J., Grosu, A., Paccini, A., Vergnaud, S., Cartus, O., Santoro, M., Fritz, S., Georgieva, I., Lesiv, M., Carter, S., Herold, M., Li, L., Tsendbazar, N.-E., … Arino, O. (2021). *ESA WorldCover 10 m 2020 v100* (Version v100) [Dataset]. Zenodo. https://doi.org/10.5281/ZENODO.5571936

Zarei, A., Hasanlou, M., & Mahdianpari, M. (2021). A comparison of machine learning models for soil salinity estimation using multi-spectral earth observation data. In Paparoditis N., Mallet C., Lafarge F., Yang M.Y., Jiang S., Shaker A., Zhang H., Liang X., Osmanoglu B., Soergel U., Honkavaara E., Scaioni M., Zhang J., Peled A., Wu L., Li R., Yoshimura M., Di K., Altan O., … Faruque F.S. (Eds.), *ISPRS Ann. Photogramm. Remote Sens. Spat. Inf. Sci.* (Vol. 5, Issue 3, pp. 257–263). Copernicus GmbH. Scopus. https://doi.org/10.5194/isprs-annals-V-3-2021-257-2021

Zhang, M., Fan, X., Gao, P., Guo, L., Huang, X., Gao, X., Pang, J., & Tan, F. (2025). Monitoring Soil Salinity in Arid Areas of Northern Xinjiang Using Multi-Source Satellite Data: A Trusted Deep Learning Framework. *Land*, *14*(1), 110. https://doi.org/10.3390/land14010110